

Turbulence, transport and their relation with the magnetic boundary in the RFX-mod device

N. Vianello, M. Agostini, A. Fassina, A. Canton, R. Lorenzini, A. Alfier, R. Cavazzana, E. Martines, P. Scarin, G. Serianni, G. Spizzo, M. Spolaore and M. Zuin
 Consorzio RFX, Associazione EURATOM-ENEA sulla Fusione, Padova, Italy

Understanding the mechanism responsible for energy and particle transport is mandatory in order to achieve better performances in fusion oriented plasmas. The discovery of H-Mode confinement regimes in Tokamaks has been accompanied by the observation of a strong reduction of plasma transport at the edge, thus fostering the effort devoted to the comprehension of edge plasma also in other magnetic configurations. The Reversed Field Pinch (RFP) is characterized by a monotonic decreasing q profile, with values always below unity, moving from around $q_0 \approx \frac{2}{3} \frac{a}{R}$ in the core to smaller negative values in the edge where the toroidal magnetic field reverses. Thus a large spectrum of $m=1$ modes is destabilized in the core whereas all the $m=0$ modes resonate at the reversal surface which is generally located few centimeters from the wall. In the same region strong density and temperature gradient have been observed [1], although a clear link between the magnetic field structure and these gradients has not been completely established. Recent numerical results revealed the existence of a chain of almost poloidally symmetric magnetic islands around the reversal surface dubbed $m=0$ islands. These islands arise because of the resonances $m=0$ modes and the beating of $m=1$ modes [2], and according to numerical simulations they influence transport properties at the edge. Apart from these characteristics which are peculiar for RFPs, the plasma outside the $q=0$ surface exhibits many analogies with other magnetic configurations. Such similarities regard for instance the particle transport, dominated by electrostatic turbulence [3], the existence of *blobs* and intermittent structures [3] and momentum transport which is found to be regulated through the electrostatic contribution to the Reynolds stress [4].

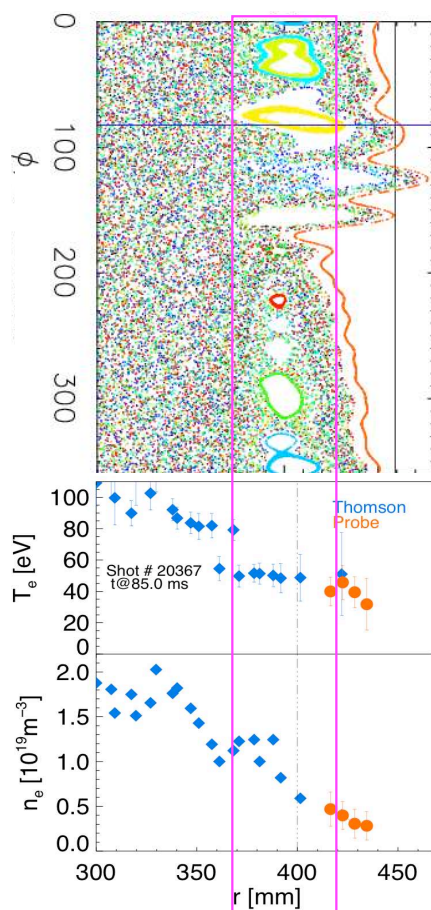


Figure 1: Upper panel. Field Line Tracing reconstruction of magnetic field, Middle panel and bottom panel: Temperature and density profile as a function of minor radius

Thus the Reversed Field Pinch edge region is a complex environment and its transport properties are determined by different concurring mechanisms. Aim of the present contribution is to describe the role played by $m=0$ islands in the formation of edge temperature and density gradients and relative transport properties and how their presence influence also the region outside the reversal surface. Data have been obtained in the RFX-Mod device, the largest RFP presently operating ($R/a = 2/0.459$ m). The first experimental observation is reported in figure 1 where temperature and density profiles as a function of minor radius are shown. Data refer to a low current Multiple Helicity discharge ($I_p = 350$ kA) with a strong reversal of the toroidal field.

In this condition higher magnetic activity is expected. These profiles have been reconstructed using both Thomson scattering data [5] (points coming from the internal profile are reported on the outward plane taking into account Shafranov shift) and probe data obtained from a complex probe which combines a radial array of 5-pin balanced triple probes.

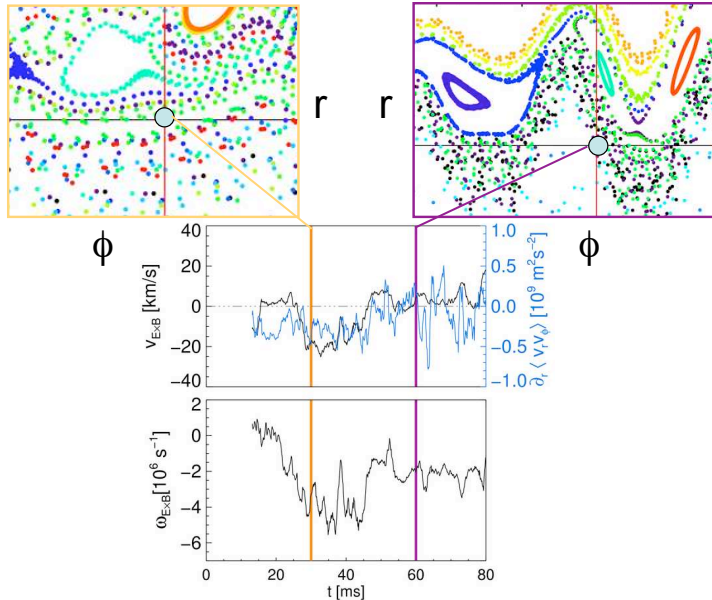


Figure 3: $\mathbf{E} \times \mathbf{B}$ and $\partial_r \langle \vec{v}_r \cdot \vec{v}_\phi \rangle$ (top) and $\omega_{E \times B}$ (bottom) as a function of time

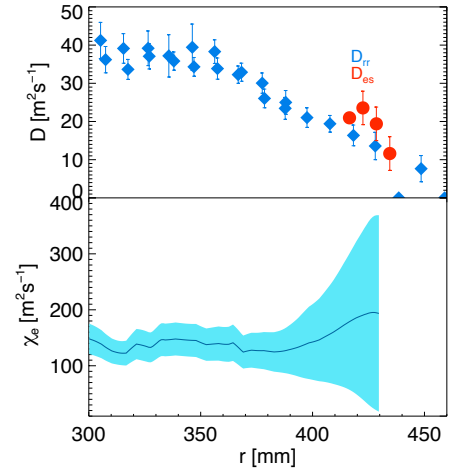


Figure 2: Upper panel. Diffusion coefficient: blue point as computed from Rechester and Rosenbluth formula, Red point as coming from electrostatic flux. Lower panel: electron thermal diffusivity

It is evident how the profile exhibits a double gradient with a plateau located in the region $360 \lesssim r \lesssim 410$ mm. In order to understand the origin of this plateau the FLiT field line tracing code [6] has been applied to the same shot. This code uses the radial profile of $m=1$ and $m=0$ modes as reconstructed by solving Newcomb's equations [7] and the resulting Poincaré plot is shown in the same figure. An horizontal line indicates the toroidal location of Thomson scattering diagnostic. The temperature plateau region corresponds to the $m=0$ island,

showing how temperature remains constant inside the island since temperature is a flux func-

tion when good magnetic surfaces are present and no heat source term exists inside the island. Using interferometer and probe data as calibration, the density profile in the same region has been obtained by using both thomson scattering and probe data. The density behavior is quite different with respect to the temperature one, with a small peak located inside the $m=0$ island. The difference in temperature and density profiles inside the $m=0$ island is easily explained taking into account that the heat source is peaked in the core, whereas the particle source is peaked in the edge resulting from the hydrogen desorbed from the wall.

The obtained profiles have been used to determine the diffusion coefficient and the electron thermal diffusivity, which are shown in figure 2. In the upper panel with red circles the diffusion coefficient as obtained from the electrostatic particle flux measured from probe is compared with the Rechester and Rosenbluth diffusion coefficient [8], which is believed to correctly describe particle diffusivity in the presence of a stochastic magnetic field. This diffusion coefficient is equal to $D(r)_{RR} = \left(\frac{\tilde{b}(r)}{B_0}\right)^2 L v_{th,i}$ with L representing an effective connection length assumed equal to the minor radius and the ion thermal velocity $v_{th,i}$

calculated assuming equal temperature for both the species. It is interesting to note how in the more external region the electrostatic contribution is found larger than the stochastic one, thus re-enforcing the analogy with tokamak where anomalous particle transport is believed to be dominated by electrostatic fluctuations. It is worth to remember that also in RFPs electrostatic transport at the edge is strongly influenced by the presence of coherent blob-like structures [3] which could account up to 50 % of particle flux at the edge. These structures are responsible for the strong non-gaussian behavior observed in the PDF of the signals [3].

As a further complication the magnetic topology influences also the $\mathbf{E} \times \mathbf{B}$ velocity and relative shear, which have a natural consequence on transport itself. An example of this behavior is shown in figure 3 where the time evolution of drift velocity and relative shear are shown as a function of time. The two colored region indicate different values of $\mathbf{E} \times \mathbf{B}$ flow and relative shear. The different behaviour can be related to a change in the magnetic topology as shown in the two Poincaré plots . In both condition a good correlation between $\mathbf{E} \times \mathbf{B}$ and Reynolds stress gradient remains, thus confirming the role of Reynolds stress in driving the flow. In order

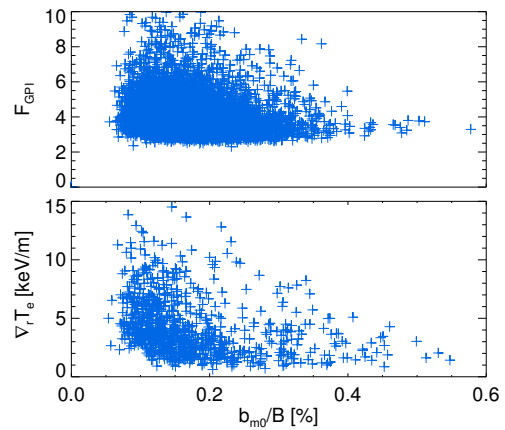


Figure 4: Top: Edge electron temperature gradient as a function of b_{m_0}/B Bottom: Flatness as computed from Gas Puff Imaging Diagnostic as a function of b_{m_0}/B

to obtain a further insight on the action of $m=0$ on the edge gradients a scaling of the edge temperature gradient as a function of normalized $m=0$ magnetic field fluctuations has been done. Numerical simulation predicts an improvement of confinement properties with the decreasing of $m=0$ fluctuations. In fact, by increasing $m=0$ fluctuations, the island width increases radially by an amount Δ proportional to the $m=0$ fluctuation amplitude; on the contrary toroidally the island width cannot increase, but the non-linear interaction with $m=1$ modes determines an erosion of the island in a chaotic layer $\sim \Delta$ wide. The experimental results are shown in the bottom panel of figure 4, where a clear increasing of edge temperature gradient is observed moving towards lower values of magnetic fluctuations. It is worth to remember that this gradient does not completely take into account the location of $m=0$ islands but has been computed for $300 \lesssim r \lesssim 400$ mm and can thus be considered as an indication of the innermost gradient. In the same plot the same scaling as been calculated for the Flatness (i.e. the 4th order momentum of the fluctuations normalized to the square of the second order one) as obtained from local emission of HeI line with the GPI diagnostic [9]. This can be taken as a rough information of the degree of intermittency, related to the presence and the intensity of blobs structures. A slight increase of this value is observed, and this can be easily explained considering that the temperature or pressure gradient reasonably represent the main source of free energy for the instabilities responsible for this type of structures.

Summarizing, in low current discharge the presence of $m=0$ islands acts in determining a temperature plateau and a density peak at the edge. This together with the observed influence on $\mathbf{E} \times \mathbf{B}$ flow and relative gradient has a direct relation with the transport properties at the edge. Different behavior is observed at higher current where improved confinement regime develops [10].

Acknowledgments This work was supported by Euratom Communities under the contract of Association between EURATOM/ENEA. The views and opinions expressed herein do not necessarily reflect those of the European Commission

References

- [1] A. Intravaia *et al* , Phys. Rev. Lett. **83**, 5499 (1999), D. Gregoratto *et al* , Nucl. Fusion **38**, 1199 (1998)
- [2] G.Spizzo *et al* , Phys. Rev. Lett. **96**, 025001 (2006)
- [3] G.Serianni *et al.*, Plasma Phys. Contr. Fusion, **49**, 2075 (2007) M. Spolaore *et al*, Phys. Rev. Lett., **93**, 215003 (2004)
- [4] N. Vianello *et al.*, Phys. Rev. Lett., **94**, 135001 (2005)
- [5] A. Alfier *et al* , Rev. Sci. Instr. **78**, 013505 (2007)
- [6] P. Innocente *et al* Nucl. Fusion **47**, 1092 (2007)
- [7] P. Zanca and D. Terranova, Plasma Phys. Contr. Fusion **46**, 1115 (2004)
- [8] A. B. Rechester and M. N. Rosenbluth, Phys. Rev. Lett. **40**, 38 (1978)
- [9] R. Cavazzana *et al* , Rev. Sci. Instr. **75**, 4152 (2004)
- [10] R. Lorenzini *et al* , "Single helical axis states in reversed field pinch plasmas", to be published in Phys. Rev. Lett..